



Luminosity, beamstrahlung energy loss and beam-beam deflections for e^+e^- and e^-e^- collisions at the ILC with 500 GeV and varying transverse beam sizes

M. Alabau Pons^{1,2}, P. Bambade¹, A. Faus-Golfe²

- 1) LAL, IN2P3-CNRS and Université de Paris-Sud, Bât.200, BP34, 91898 Orsay Cedex
- 2) IFIC, Edificio Institutos de Paterna, Aptdo. 22085, 46071 Valencia, Spain

Abstract

At the interaction point of the International Linear Collider, beam-beam effects due to the strong electromagnetic fields that the bunches experience during collisions cause a mutual focusing, called pinch effect, which enhances the luminosity in the case of e^+e^- collisions. The opposite is true for e^-e^- collisions. In this case the luminosity is reduced by mutual defocusing, or anti-pinching. The resulting beamstrahlung energy loss and beam-beam deflection angles as function of the vertical transverse offset are also different for both modes of operation. The dependence of these quantities with transverse beam sizes are presented for the case of e^-e^- collisions.

1 Introduction

At the interaction point (IP) of the International Linear Collider (ILC), beam-beam effects due to the strong electromagnetic fields that the bunches experience during collisions cause a mutual focusing, called pinch effect, which enhances the luminosity in the case of e^+e^- collisions. The opposite is true for e^-e^- collisions. In this case the luminosity is reduced by mutual defocusing, or anti-pinching.

Another difference between the two modes of operation is the much steeper dependence of the beam-beam deflection angle with respect to transverse beam offsets at the IP, for e^-e^- collisions in comparison with e^+e^- . The resulting observable is known to be less favourable for the fast intra-train feedback system used to maintain the beams in collision at the IP [1]. Moreover, the luminosity drops much more rapidly with increasing transverse offsets for e^-e^- as compared with e^+e^- , which implies tighter feedback requirements for the latter.

One way to recover a useful capture range and easier conditions for the feedback system is to specify somewhat rounder beams for e^-e^- collisions. This has however the disadvantage that peak luminosity is reduced and that the centre-of-mass energy dilution due to beamstrahlung is enhanced.

In an optimization, the average luminosity performance of the planned feedback system needs to be analysed for the e^-e^- case using the same assumptions as for e^+e^- , in order to specify the maximum steepness allowed for the beam-beam deflection curve. The beam parameters can then be adjusted to satisfy this constraint while keeping the average energy dilution due to beamstrahlung below reasonable values, as required to satisfy the optical band-pass of the post-IP extraction system and for the purpose of measuring mass thresholds precisely.

Changing the demagnification of the final focus optics towards rounder beams may also be necessary in the 2mrad crossing angle geometry [2], to enable extracting the spent beam in the case of e^-e^- collisions.

In this note, a comparison of the dependence with transverse beam sizes of the luminosity, beamstrahlung energy loss and beam-beam deflection angles in the e^+e^- and e^-e^- collision modes is presented. This will serve as input to the optimisation of beam parameters for the e^-e^- case.

A centre-of-mass energy of 500 GeV and the nominal [3] beam parameters in Table 1 are used. The study is carried out simulating beam-beam collisions with the GUINEA-PIG [4] program and using idealised Gaussian beam distributions.

Table 1: Main ILC beam parameters with 500 GeV centre-of-mass energy.
The nominal beam parameters described in [3] are shown.

Beam Parameter	Nominal 500
Beam Energy (GeV)	250
Repetition Rate (Hz)	5
Bunch Charge	$2.0 \cdot 10^{10}$
Bunches per rf pulse	2820
Bunch spacing (ns)	307.7
$\gamma\epsilon_x$ (m-rad)	$1000 \cdot 10^{-8}$
$\gamma\epsilon_y$ (m-rad)	$4.0 \cdot 10^{-8}$
β_x (mm)	21
β_y (mm)	0.40
σ_x (nm)	655
σ_y (nm)	5.7
σ_z (μm)	300
Geometric Luminosity ($\text{cm}^{-2}\text{s}^{-1}$)	$1.2 \cdot 10^{34}$
Luminosity ($\text{cm}^{-2}\text{s}^{-1}$)	$2.03 \cdot 10^{34}$

2 Comparison between e^+e^- and e^-e^- collisions for ILC with nominal parameters

The luminosities obtained for different vertical offsets in e^+e^- and e^-e^- collisions using nominal ILC beam parameters are shown in Figure 1. The luminosity at zero offset for e^-e^- collision is about 20% of that for e^+e^- . This reduction is due to the anti-pinch effect. The luminosity also drops more rapidly with relative vertical offset for e^-e^- than for the e^+e^- .

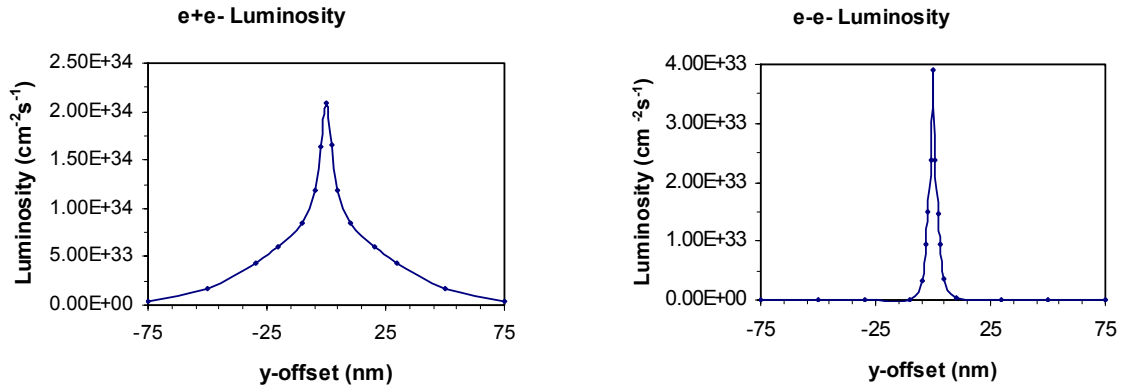


Figure 1: Luminosity versus vertical offset for e^+e^- and e^-e^- collisions at the ILC with nominal parameters at 500 GeV in the centre-of-mass.

Figure 2 shows the vertical deflection angles for beam 1 obtained for different vertical offsets for e^+e^- and e^-e^- collisions. The slope of the deflection curve in e^-e^- collisions is approximately 10 times that for the e^+e^- case.

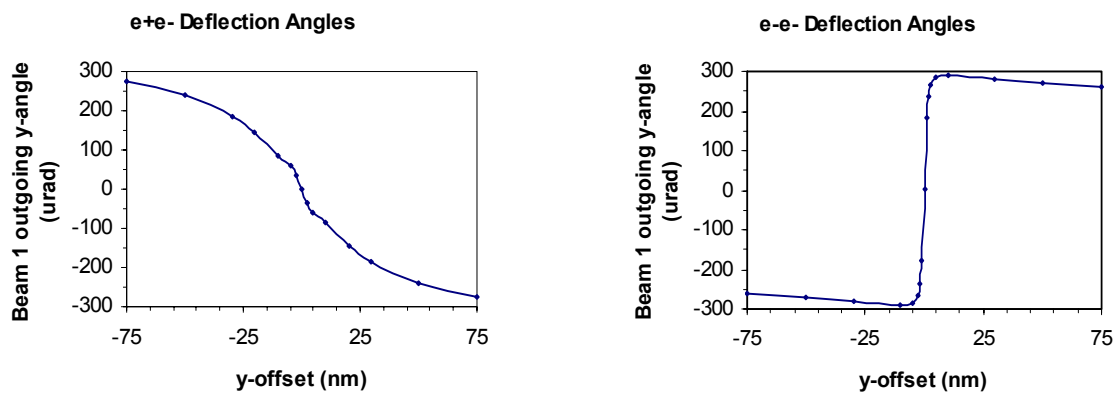


Figure 2: Vertical deflection angle (beam 1) versus vertical offset for e^+e^- and e^-e^- collisions at the ILC with nominal parameters at 500 GeV in the centre-of-mass.

The beamstrahlung energy loss is slightly smaller for e^-e^- collisions as compared to e^+e^- , but still rather similar. This is shown in Figure 3.

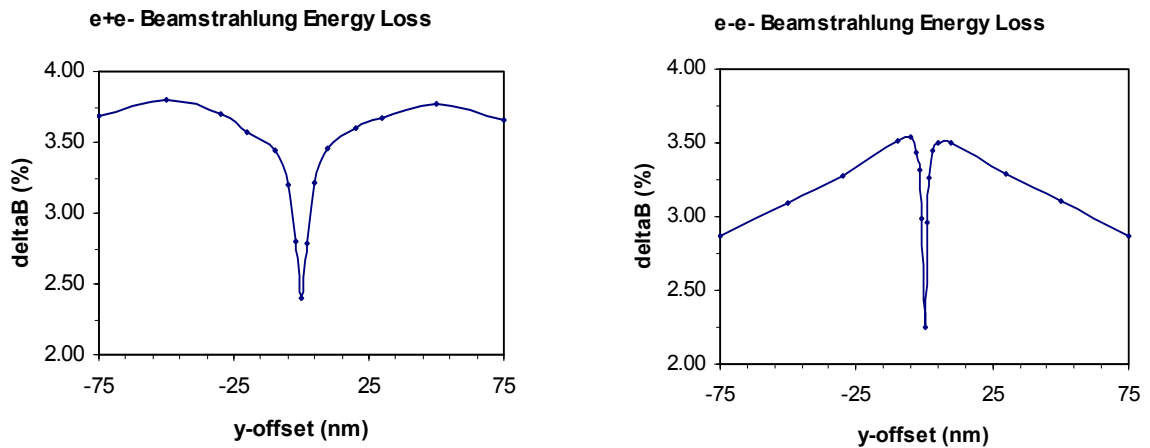


Figure 3: Beamstrahlung energy loss versus vertical offset for e^+e^- and e^-e^- collisions at the ILC with nominal parameters at 500 GeV in the centre-of-mass.

3 Different vertical beam sizes for e^-e^- collision with a nominal horizontal beam size

The luminosity, deflection angles and beamstrahlung energy loss for e^-e^- collision are shown in Figures 4, 5 and 6, respectively, for increasing vertical beam sizes, keeping the nominal value for the horizontal size.

If the vertical beam size is increased by a factor five, a more slowly varying beam-beam deflection curve is obtained while the beamstrahlung energy loss remains similar. The luminosity is reduced by a factor two in this case.

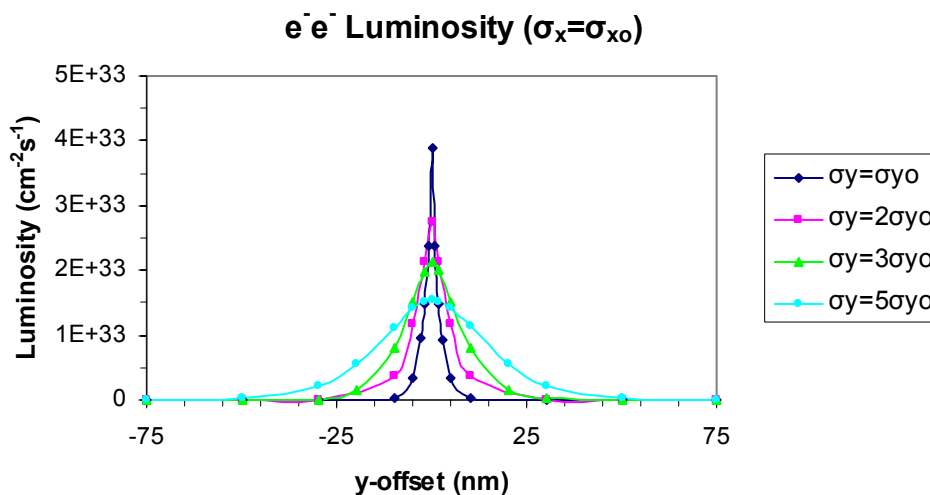


Figure 4. Luminosity versus vertical offset for e^-e^- collisions with increased vertical beam sizes.

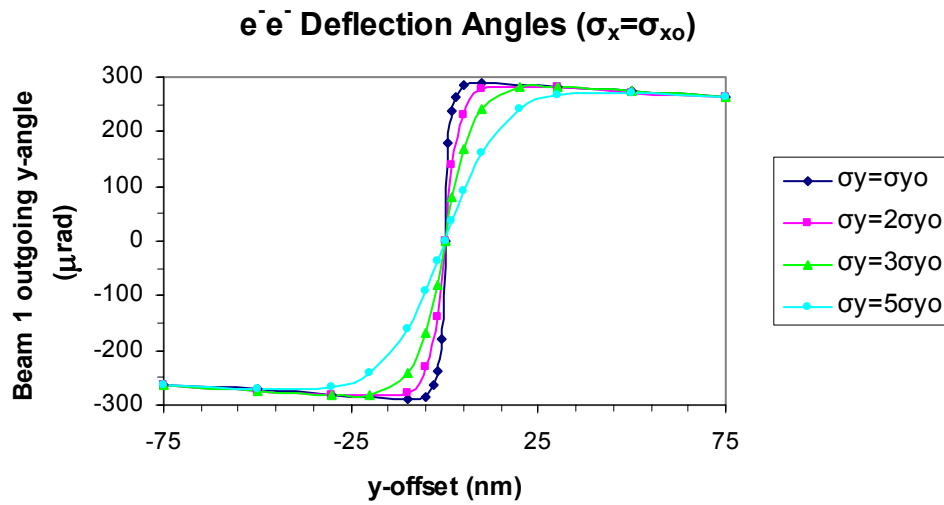


Figure 5. Deflection angle versus vertical offset for e^-e^- collisions with increased vertical beam sizes.

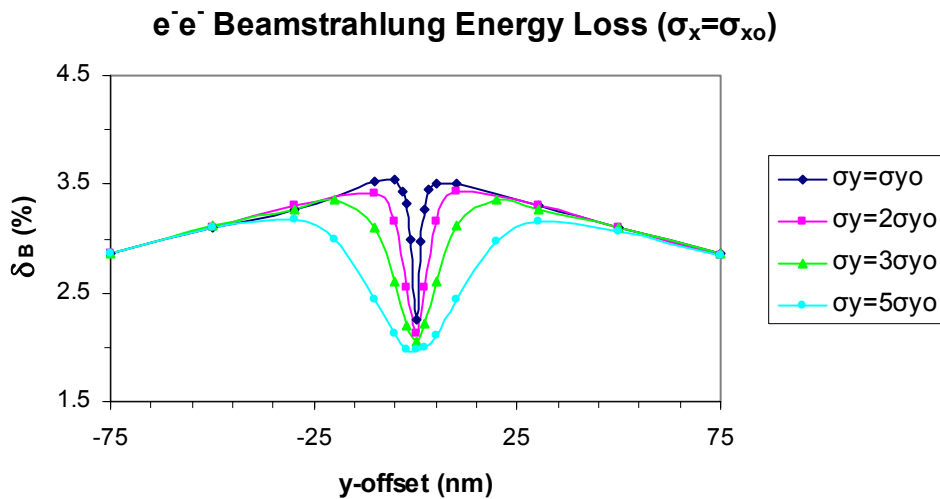


Figure 6. Beamstrahlung energy loss versus vertical offset for e^-e^- collisions with increased vertical beam sizes.

Figure 7 shows the luminosity for zero vertical offset versus σ_x/σ_y . The nominal value for the σ_x/σ_y ratio is marked with a circle and is approximately 115.

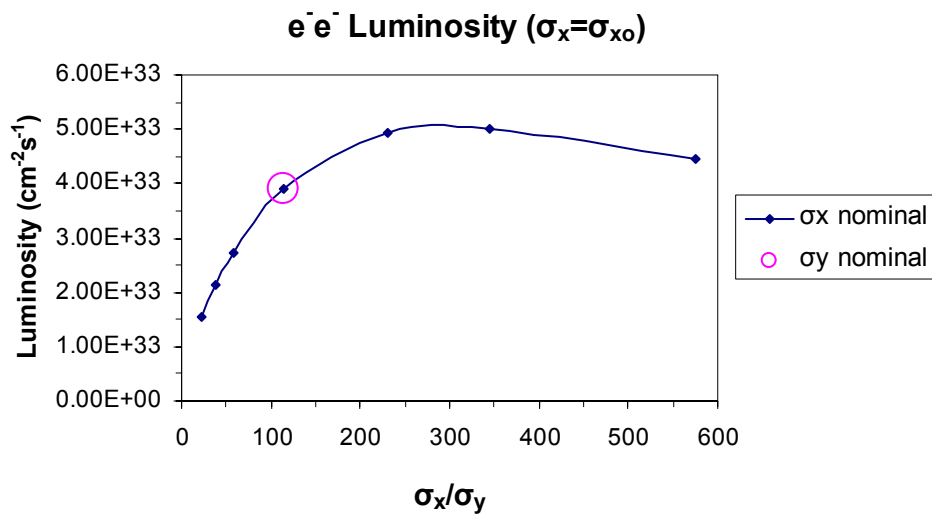


Figure 7. Luminosity versus σ_x/σ_y for e^-e^- collisions with a nominal horizontal beam size.

The luminosity increases slightly and then drops again when the vertical beam size is decreased below the nominal value (increasing the σ_x/σ_y ratio). This is due to the hour-glass effect (see the description in the Appendix).

Figure 8 shows the slope of the deflection curve versus the σ_x/σ_y ratio. The slopes becomes steeper when the vertical beam size is decreased and are much larger than the typical value for e^+e^- collisions (about $6\mu\text{rad}/\text{nm}$) shown in Figure 2.

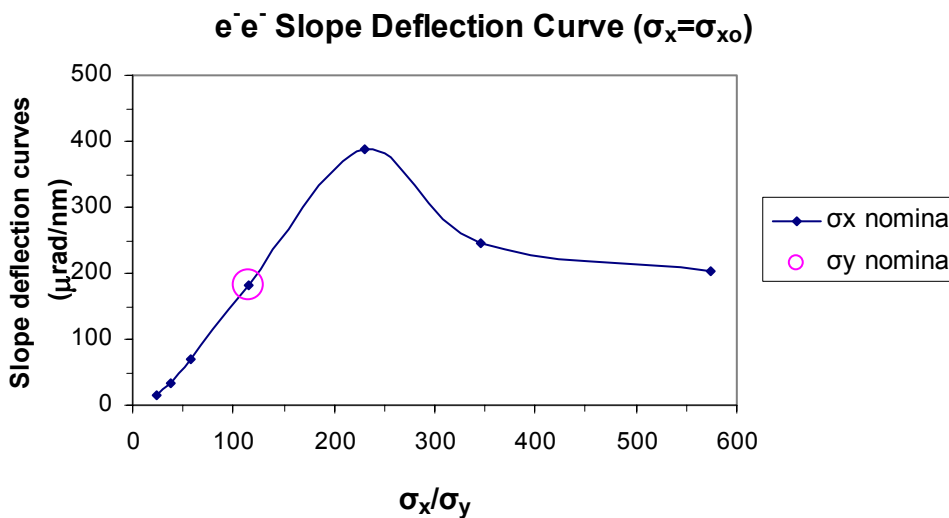


Figure 8. Slope of the deflection curves versus σ_x/σ_y ratio for e^-e^- collisions with a nominal horizontal beam size.

Figure 9 shows the beamstrahlung energy loss for zero vertical offset versus σ_x/σ_y .

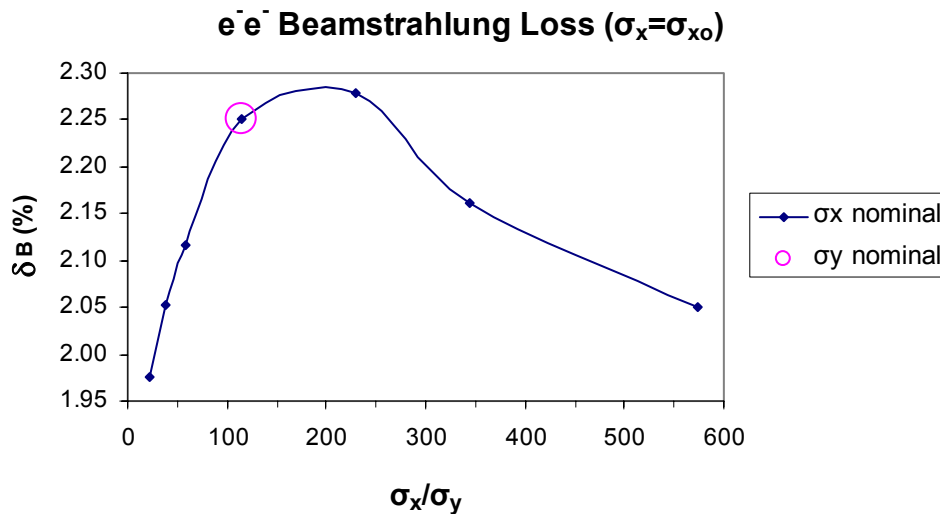


Figure 9. Beamstrahlung energy loss versus σ_x/σ_y for e^-e^- collisions with a nominal horizontal beam size.

4 Different horizontal beam sizes for e^-e^- collision while keeping the nominal vertical beam size

The luminosities and beamstrahlung energy loss for zero vertical offset and the slope of the deflection curves versus σ_x/σ_y ratio are shown in Figures 10, 11 and 12, respectively, for horizontal beam sizes decreased by factor of 5 and 10. The value of the σ_x/σ_y ratio for nominal beam sizes (marked with a circle) is approximately 115.

Decreasing the horizontal beam size while keeping the vertical one at the nominal value increases the luminosity as can be seen in Figure 10. However, the beamstrahlung energy loss then increases significantly and the deflection curves become steeper (see Figures 11-12). For comparison, the slope of the deflection curve for e^+e^- collisions is approximately $6\mu\text{rad/nm}$, as was shown in Figure 2.

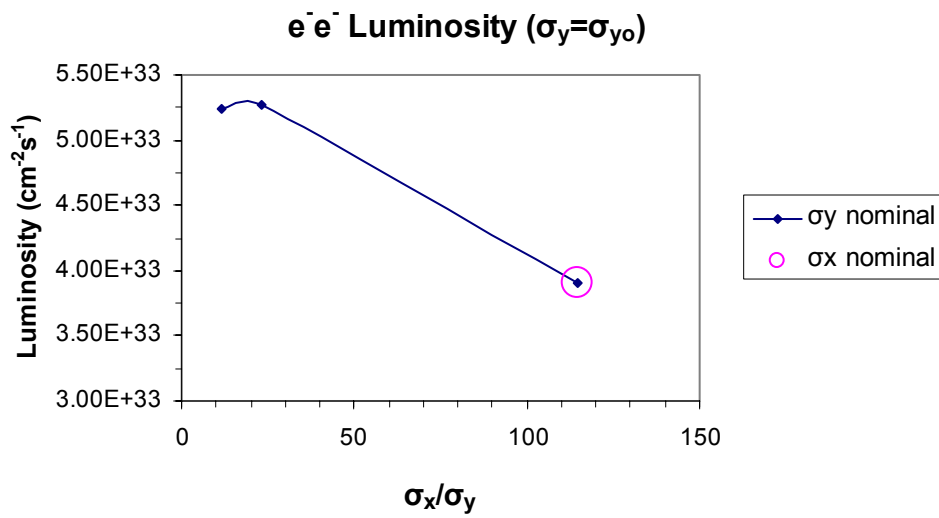


Figure 10. Luminosity versus σ_x/σ_y ratio for e^-e^- collisions with a nominal vertical beam size. The rise at the lowest values of σ_x/σ_y turns over as the hour glass effect (described in the Appendix) becomes important in the horizontal plane when $\beta_x < \sigma_z$.

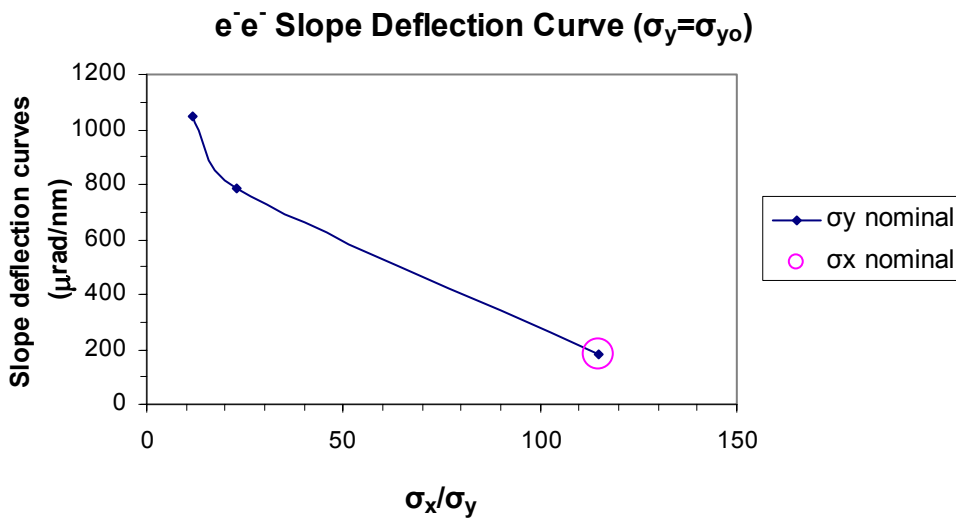


Figure 11. Slope of the deflection curves versus σ_x/σ_y ratio for e^-e^- collisions with a nominal vertical beam size.

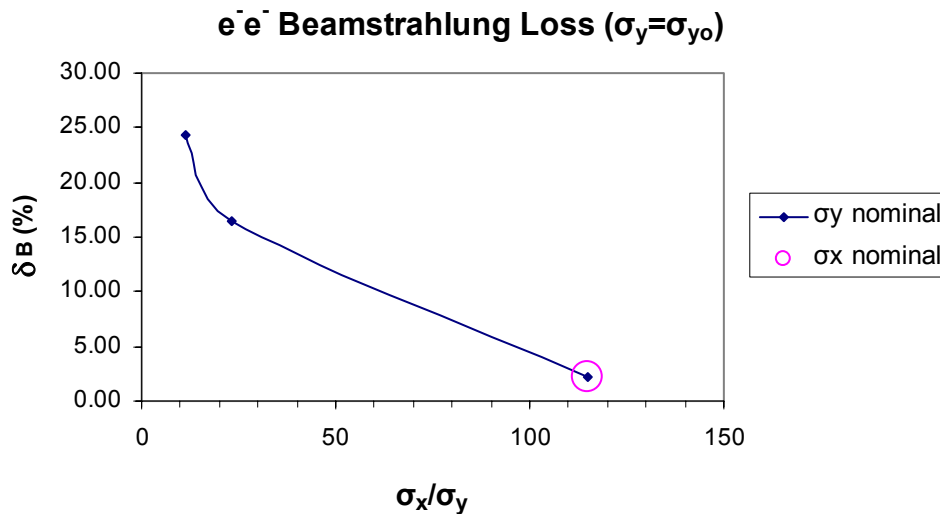


Figure 12. Beamstrahlung energy loss versus σ_x/σ_y ratio for e^-e^- collisions with a nominal vertical beam size.

5 Different horizontal and vertical beam sizes for e^-e^- collisions

As have been seen in Sections 3 and 4, increasing the vertical beam size gives a gentler slope for the deflection curve, but the luminosity decreases. On the other hand, if the horizontal beam size is decreased, the luminosity increases, but the deflection curve becomes steeper and the beamstrahlung energy loss increases. In this section, both beam sizes are varied simultaneously to find a compromise for the three quantities, the goal being to achieve gentler deflection curves with moderate luminosity and beamstrahlung energy losses at zero offset.

5.1 Different horizontal beam sizes for a vertical beam size 10 times the nominal one

The luminosity, deflection angles and beamstrahlung energy loss are shown in Figures 13, 14 and 15, respectively, for different horizontal beam sizes increasing the vertical one 10 times with respect to the nominal value ($\sigma_y=57.0\text{nm}$). Decreasing at the same time the horizontal beam size 10 times ($\sigma_x=65.5\text{nm}$) the beam becomes approximately round.

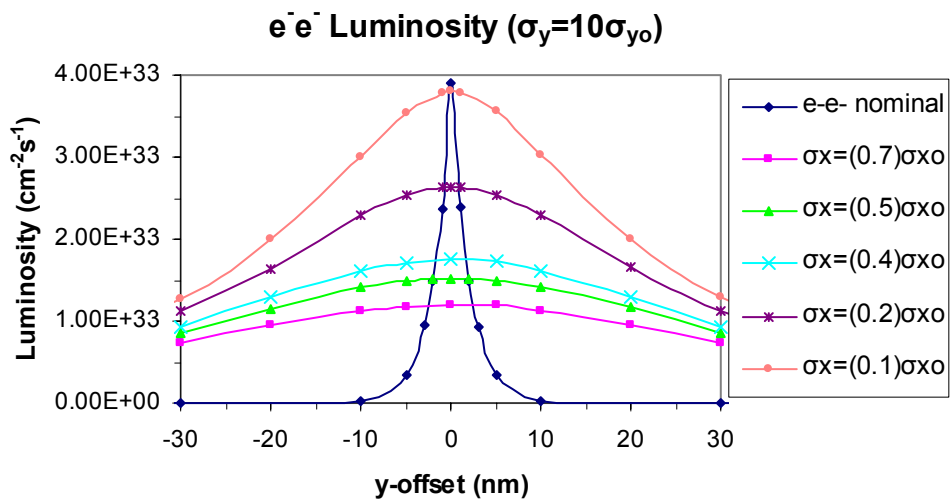


Figure 13. Luminosity versus vertical offset for different horizontal beam sizes and the vertical beam size 10 times the nominal.

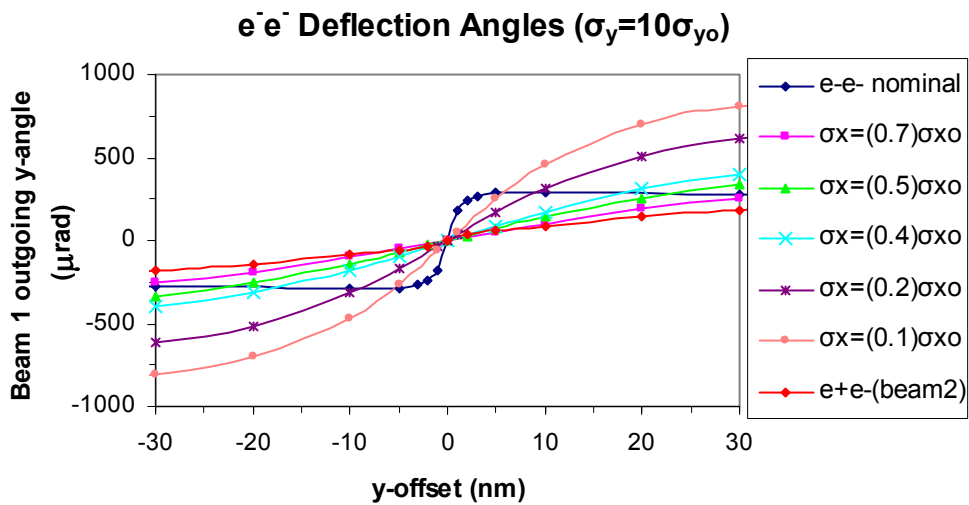


Figure 14. Deflection angle versus vertical offset for different horizontal beam sizes and the vertical beam size 10 times the nominal.

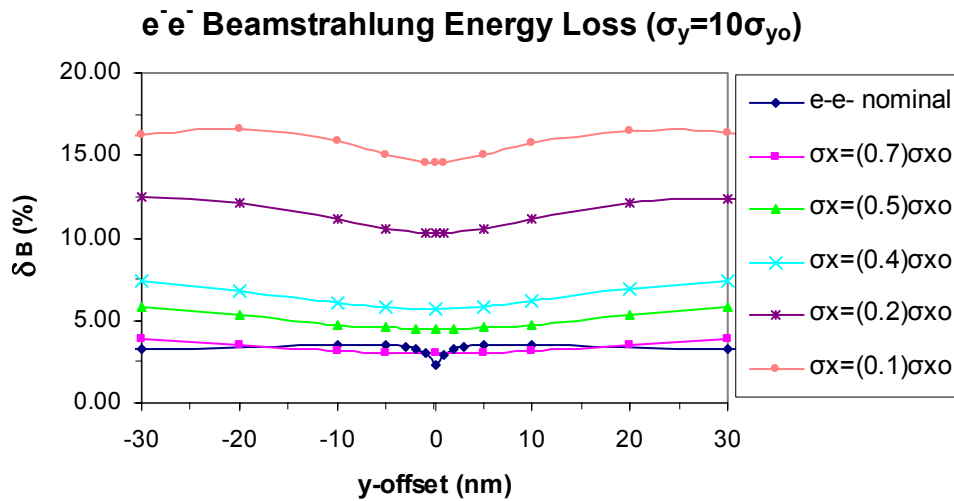


Figure 15. Beamstrahlung energy loss versus vertical offset for different horizontal beam sizes and the vertical beam size 10 times the nominal.

In Figure 13 can be seen that for an approximately round beam the maximum luminosity is rather similar to the nominal one while the deflection curve is less steep than for the nominal case (Figure 14). But as can be seen in Figure 15, the beamstrahlung energy loss becomes much too large in this case.

5.2 Different vertical beam sizes for a horizontal beam size half the nominal one

Figures 16, 17 and 18 show, respectively, the luminosity, deflection angles and beamstrahlung energy loss for different vertical beam sizes and a horizontal beam size half that of the nominal value ($\sigma_x = 327.5\text{nm}$). In this case, gentler deflection curves can be obtained by increasing the vertical beam size at the expense of only a moderate reduction in luminosity at zero offset and a somewhat increased beamstrahlung energy loss.

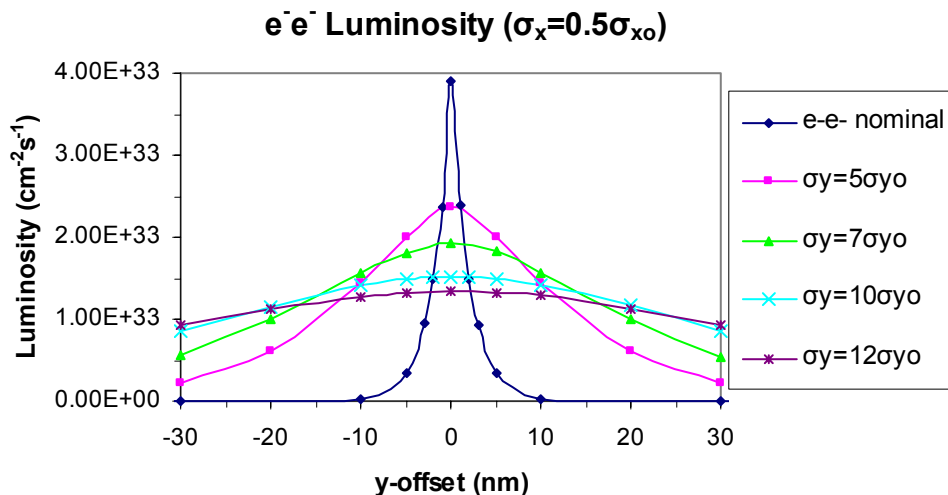


Figure 16. Luminosity versus vertical offset for different vertical beam sizes and a horizontal beam size half the nominal.

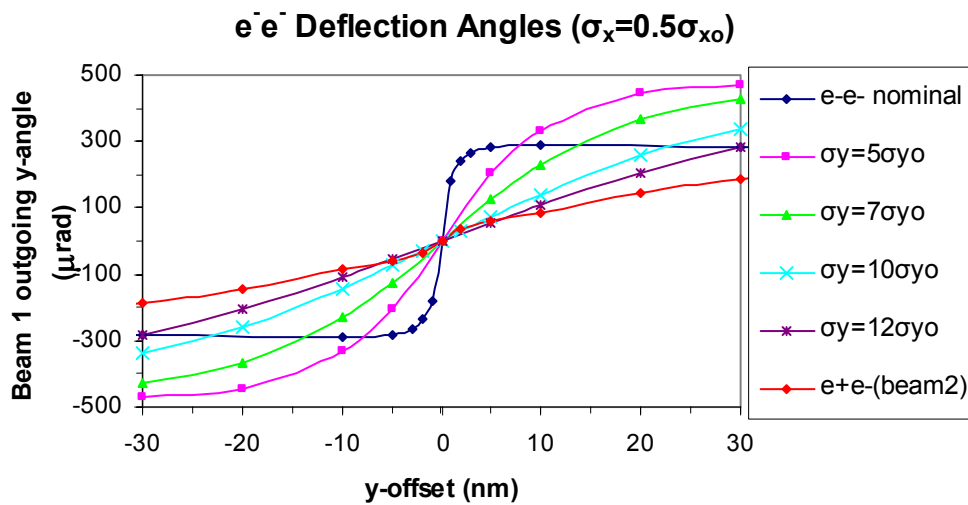


Figure 17. Deflection angle versus vertical offset for different vertical beam sizes and a horizontal beam size half the nominal.

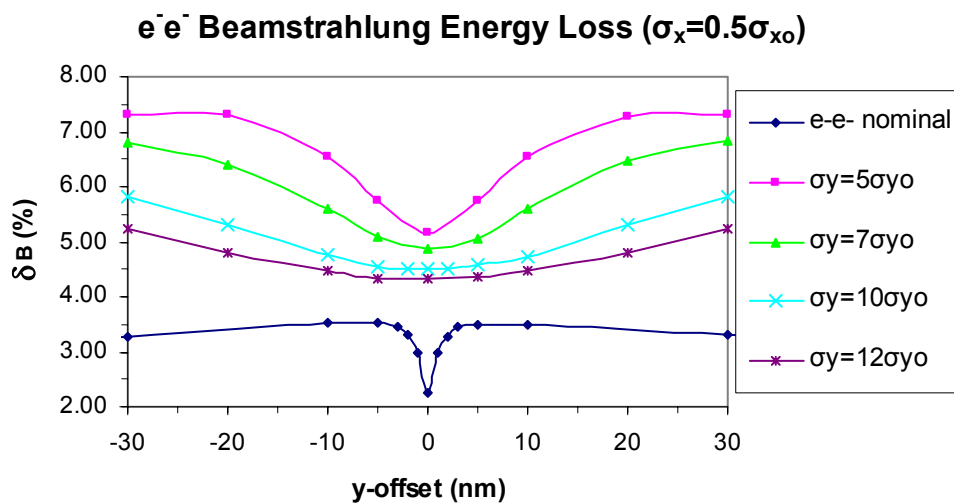


Figure 18. Beamstrahlung energy loss versus vertical offset for different vertical beam sizes and a horizontal beam size half the nominal.

6 Conclusions and further work

Increasing the vertical beam size by a factor 5, the steepness of the deflection curve can be reduced, but this is at the expense of a factor 2 in luminosity at zero offset. This luminosity reduction can be recovered partly by decreasing the horizontal beam size. In this case, an even gentler deflection curve is obtained, but at the expense of a factor 2 larger beamstrahlung energy loss. Deflection curves rather similar to the e^+e^- case can for instance be obtained with a beamstrahlung energy loss of 5% (instead of 2% for nominal beam parameters).

A final optimisation must await a study of the performance of the feedback system, to compute the average luminosities obtained for the different beam parameter sets, taking into account assumptions similar to those implemented for the case of e^+e^- collisions. Such a study is underway.

To complement this study, it will also be checked that the final focus optics has enough flexibility to adjust smoothly (using the same magnets and within their planned operational ranges) for the different beam parameters which may be needed for e^+e^- and e^-e^- . This is fairly easy for the 20mrad and 14mrad crossing angle geometries, but more involved for e^-e^- in the 2mrad case, because the last (defocusing) quadrupole is shared by the incoming and outgoing beams in this scheme, with the outgoing beam transported off-axis as part of its extraction [5]. A suggested solution [2] to accommodate e^-e^- in this scheme is to reverse the standard focusing-defocusing final doublet sequence for this specific case. This should be easier with the rounder beams which may be needed for e^-e^- .

Finally, the impact of the larger beamstrahlung centre-of-mass energy dilution will need to be assessed, both from the point of view of the performance of the post-IP extraction line, and to analyse the degradation in mass resolution which can result in threshold measurements of scalar lepton pair production, for which the e^-e^- option is thought to be superior to the regular e^+e^- mode.

Acknowledgements

We acknowledge the support of the European Community Research Training Network programme under FP5 (PROBE FOR NEW PHYSICS, contract number RTN2-2001-00450) and of the European Community Research-Infrastructure and Activity under the FP6 "Structuring the European Research Area" programme (CARE, contract number RII3-CT-2003-506395).

References

- [1] I. Reyzl and S. Schreiber, International Journal of Modern Physics A Vol. 15 No. 15 (2000) 2495-2505.
- [2] A. Seryi, Running 2mrad IR in the e^-e^- mode: BDS constraints. Presented at Snowmass, August 2005.
- [3] T. Raubenheimer, "Suggested ILC Beam Parameter Range", February 2005, <http://www-project.slac.stanford.edu/ilc/acceldev/beampar/Suggested%20ILC%20Beam%20Parameter%20Space.pdf>.
- [4] D. Schulte, Ph.D. thesis, University of Hamburg 1996, TESLA-97-08.
- [5] R. Appleby, D. Angal-Kalinin, P. Bambade, B. Mouton, O. Napoly and J. Payet, "Alternative IR geometries for TESLA with a small crossing angle", hep-ex/0412026

Appendix*

In the case of bunches with Gaussian distributions in both horizontal and vertical planes, the luminosity can be expressed as

$$L = \frac{n_b N_b^2 f_{rep}}{4\pi\sigma_x^* \sigma_y^*} H_D$$

where n_b , N_b , f_{rep} , $\sigma_{x,y}^*$ and H_D are, respectively, the number of bunches per train, the number of particles per bunch, the repetition train, the transverse beam sizes at the IP and the pinch enhancement factor (or anti-pinch reduction factor for e^-e^- collisions). H_D can be approximated by the following expression

$$H_{D_{x,y}} = 1 + D_{x,y}^{1/4} \left(\frac{D_{x,y}^3}{1 + D_{x,y}^3} \right) \left[\ln(\sqrt{D_{x,y}} + 1) + 2 \ln\left(\frac{0.8\beta_{x,y}}{\sigma_z} \right) \right]$$

where $\beta_{x,y}$ are the β -functions at the IP and $D_{x,y}$ are the so-called disruption parameters, given by

$$D_{x,y} = \frac{2r_e N_b \sigma_z}{\gamma\sigma_x(\sigma_x + \sigma_y)}$$

where r_e and γ are the classical electron radius and relativistic factor, respectively. The last term in the expression of the enhancement/reduction factor comes from the so-called hour-glass effect and is responsible for the luminosity drop when $\beta_{x,y} < \sigma_z$.

* Nick Walker, "Beam-Beam Effects", USPAS, Santa Barbara, June 2003
(see <http://www.desy.de/~njwalker/uspas/>)